

## Stark spectroscopy and Autler-Townes interactions in four-level cesium atoms

John E. Wessel\* and Donald E. Cooper†

*Chemistry and Physics Laboratory, The Aerospace Corporation, El Segundo, California 90254*

(Received 11 August 1986)

Scalar and tensor polarizabilities of cesium  $5f$  and  $7d$  states were measured by three-color multiphoton excitation techniques. The low-field results were quadratic and were in good agreement with calculated values. The oscillator strength for the  $5f$ - $5g$  transition was measured to be  $0.0336 \pm 0.0003$ , in close agreement with theory. At higher electric fields, we clearly resolved Autler-Townes avoided crossings between  $5f$  levels and dressed  $7d$  states. The observed doublet-component separations scaled linearly with Rabi frequency for the  $7d$ - $5f$  transitions, supporting a two-level model for the four-level experiment. The results are interesting because the observed spectra were independent of Rabi frequencies for the  $6s$ - $6p$  and  $6p$ - $7d$  transitions. Angular momentum forbidden transitions from  $7d$ ,  $J_z = \frac{1}{2}$  to  $5f$ ,  $J_z = \frac{5}{2}$  were observed at higher dc fields. These are attributed to dc-field-induced mixing between nearly degenerate  $5f$  and  $5g$  states.

### INTRODUCTION

Laser sources have greatly extended studies of excited atomic states. The early work provided accurate data on atomic polarizabilities and subsequent investigations revealed interesting new behavior in the regime of strong external electric field quantized Rydberg states. More recently, significant advances have been made in understanding radiative interactions in the regime where the external electromagnetic field influences quantization and dominates decay processes. Currently there is considerable interest in the effect of Autler-Townes interactions on coherent excitation of multilevel systems.<sup>1,2</sup>

In this paper we present results from multiphoton-excitation experiments with three- and four-level cesium under conditions of moderately strong static electric and optical fields. In prior work ultrahigh-resolution laser spectroscopy of two- and three-level alkali atoms was employed to confirm the dressed-atom model of Burshtein,<sup>3,4</sup> Newstein,<sup>5</sup> and Mollow<sup>6</sup> for strong-field radiative interactions with a two-level atom. Two-component absorption and three-component fluorescence emission were predicted for a two-level atom. The experimental confirmation of theory by Schuda, Stroud, and Hercher,<sup>7</sup> by Walther and co-workers,<sup>8,9</sup> and by Ezekiel and co-workers<sup>10,11</sup> represented a major advance in understanding the interactions between intense coherent laser sources and atomic transitions. Subsequent experiments confirmed predictions of two-component probe absorption bands for strongly pumped two-level atoms. Picque and Pinard<sup>12</sup> observed doublet absorption lines for a weak probe beam incident on sodium in an atomic beam with two-level pumping of the  $D_2$  transition. The weak probe beam interrogated the  $3p_{3/2}$ - $5s_{1/2}$  transition, revealing doublet structure. Whereas the above work was performed in atomic beams, Delsart and Keller<sup>13</sup> were able to observe similar effects in a static cell using neon strongly pumped between the  $1s_5$  and  $2p_4$  states. They probed a weak tran-

sition originating from the  $2p_4$  state and observed a well-resolved Autler-Townes splitting. In subsequent work, Gray and Stroud<sup>14</sup> explored the resonant three-level optical interactions in the case of strong pump and probe beams for the sodium  $3s$ - $3p$ - $4d$  transition. The results were well described by two-level theory, adapted to the three-level atom in a strong field. This theory predicted that the doublet, observed for a low-intensity probe beam, would broaden and fill in at center frequencies, for a high-power probe beam. A complicated density-matrix treatment was required to predict the line shape. The results confirmed the validity of this treatment for high-intensity excitation of a three-level system.

Isolation of nondegenerate levels is an important refinement required for studies of the Autler-Townes effect. In prior work, the predicted line shapes could not be verified until techniques of optical pumping or Stark shifting were introduced to suppress effects of magnetic quantum-state degeneracy. In the experiments we report this condition was achieved as a result of the strong Stark interaction in the final state. Thus, even though we use a static thermal atomic vapor cell, the four-level excitation experiments isolate specific  $J_z$  levels. Sub-Doppler excitation is achieved by the resonant narrow line conditions.

The primary emphasis of this report is on Stark spectroscopy of cesium  $7d$  and  $5f$  levels. This follows a great deal of prior work on alkali-metal  $d$  and  $f$  states. In prior work<sup>15</sup>  $f$  states were populated by spontaneous transitions from more-energetic  $d$  states, excited by two-photon absorption. These latter studies employed an atomic beam in order to reduce Doppler broadening. In another study<sup>16</sup> polarizabilities of high principal quantum number  $s$ ,  $p$ ,  $d$ , and  $f$  states of potassium were measured by laser-microwave double resonance, combined with detection by field ionization. This led to extensive work in the area of field-ionization spectroscopy of Rydberg states. These prior studies provided values for scalar ( $\alpha_0$ ) and/or tensor ( $\alpha_2$ ) polarizabilities in a number of excited alkali-metal

states. Data are far from complete, and there are no reported values for polarizability of the cesium  $5f$  state, nor have values been reported for tensor polarizability in the  $7d$  state of cesium. Cesium is a particularly interesting case, in that  $\alpha_0$  is expected to be  $J$  dependent due to the substantial spin-orbit interaction. Previously,  $\alpha_0$  was found to be independent of  $J$  for  $p$  and  $d$  states of sodium and potassium. In cesium the measured values for polarizability will provide a test of refined heavy-atom wave functions.

We report new observations involving two- and three-photon excitation of cesium between  $6s$ ,  $6p$ ,  $7d$ , and  $5f$  states, as shown schematically in Fig. 1. The work provides the first reported observation of Autler-Townes splitting in a four-level system. The results are easily interpreted in terms of a two-level interaction involving the  $7d$  and  $5f$  states, even though the comparably strong  $6s$ - $6p$  and  $6p$ - $7d$  transitions are simultaneously pumped. The  $5f$  state is representative of the intermediate angular momentum regime, where the external electric field induces weak, but noticeable, changes in quantization. In the course of this work scalar and tensor polarizabilities were measured for the  $7d$  and  $5f$  states, providing an accurate check of previously calculated values. A new electric-field-induced transition mechanism was observed in four-level tuning studies. It violates zero-field constraints on angular momentum changes in dipole transitions. Both this effect, and the measured  $5f$  polarizability, are readily interpreted in terms of the near-resonance interaction between  $5f$  and  $5g$  states.

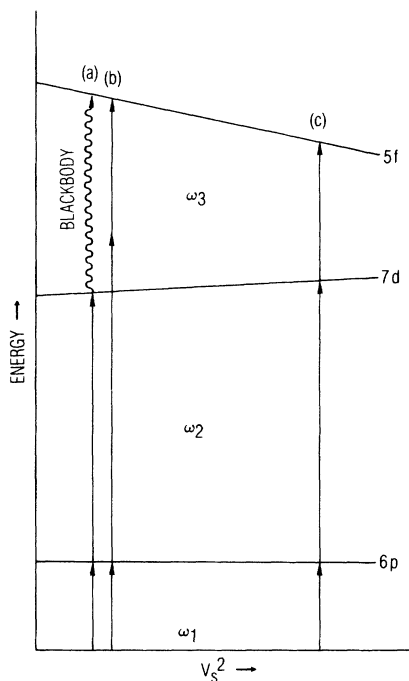


FIG. 1. Schematic energy-level diagram showing the influence of electric field on resonance conditions for fixed excitation frequencies,  $\omega_1$  and  $\omega_3$ .

## EXPERIMENTAL PROCEDURE

Measurements were performed using two single-mode tunable cw dye lasers and one line-tunable cw  $\text{CO}_2$  laser, in the geometry described in Fig. 2. Laser-wavelength scans were calibrated against a reference étalon with 2.0-GHz free spectral range and finesse of 100. The cesium was contained in a static cell equipped with three sapphire windows (oriented for the desired polarization conditions) for laser access and fluorescence collection, and one  $\text{BaF}_2$  window for  $\text{CO}_2$  laser access. The electric field was applied by a pair of 2.5-cm-diameter flat, parallel electrodes spaced by  $0.493 \pm 0.001$  cm. Voltages were measured with an accuracy of about 0.1%. Excitation was monitored by detecting fluorescence from either the Cs  $5f$ - $5d$  or  $8p$ - $6s$  transition, depending on experimental conditions. The  $6s$ - $6p$ - $7d$  transition was excited in the counterpropagating configuration, thus suppressing Doppler broadening. At low laser power, additional linewidth reduction was observed due to velocity selection in the  $6s$ - $6p$  transition. Optical pumping of the atomic population away from the resonant hyperfine transition was minimized by tuning the  $6s$ - $6p$  excitation source to the high-frequency edge of the low-frequency hyperfine transition or to the low-frequency edge of the high-frequency transition. Experimental conditions permitted resolution approaching 10 MHz, which was more than adequate to measure Stark tuning curves and to observe intensity dependence of Autler-Townes splitting for moderately low laser intensities. Resolution was inadequate to measure hyperfine structure in the  $f$  manifold.

## RESULTS

We discuss, in sequence, results for  $7d$  Stark spectroscopy,  $5f$  Stark spectroscopy, observation of Autler-Townes effects, and observation of dipole-forbidden transitions in cesium.

### $7d$ spectroscopy

Spectral scans were recorded by sweeping the  $\omega_2$  laser across  $7d$  and  $5f$  resonances while holding the dc electric field and  $\text{CO}_2$  laser-frequency constant. Blackbody radiation induced the  $5f$ - $5d$  fluorescence detected subsequent to  $7d$  excitation, whereas  $5f$  excitation generated fluorescence directly. Results for  $7d_{5/2}$  are shown in Fig. 3. Measurements were performed on both the  $7d_{3/2}$  and  $7d_{5/2}$  states. Tuning curves were quadratic, within accuracy of measurement, over the ranges studied. Com-

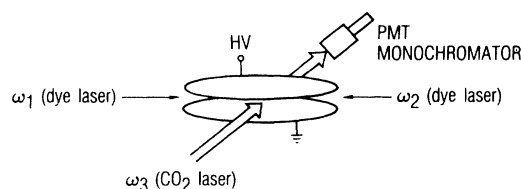


FIG. 2. Experimental configuration.

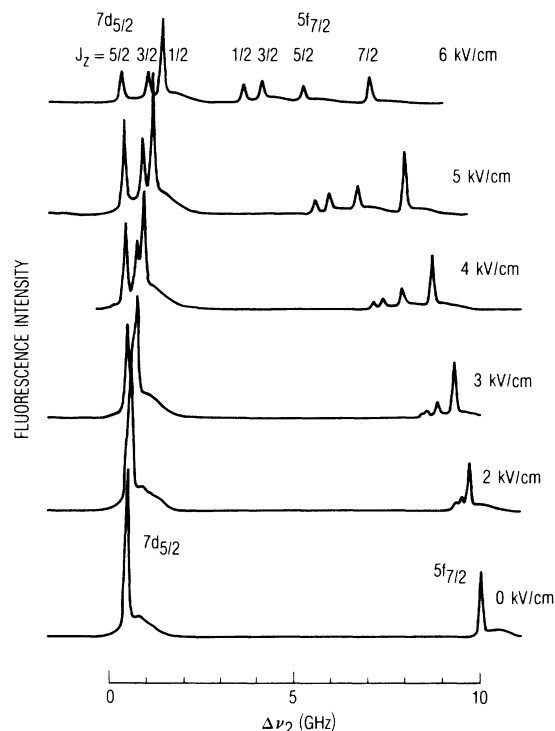


FIG. 3. Spectral scans recorded as a function of  $\nu_2$  for the overall transition  $6s_{1/2} \rightarrow 6p_{3/2} \rightarrow 7d_{5/2} \rightarrow 5f_{7/2}$ , detected by  $5f \rightarrow 5d$  fluorescence. The individual scans correspond to applied electric fields ranging from 0 to 6 kV/cm. Detection gain was reduced by a factor of 3 for the scan at 6 kV/cm.

ponents corresponding to  $J_z = \frac{3}{2}$  and  $J_z = \frac{1}{2}$  were observed for  $7d_{3/2}$  and components with  $J_z = \frac{5}{2}, \frac{3}{2},$  and  $\frac{1}{2}$  were observed for the  $7d_{5/2}$  state. Polarization conditions were selected to reveal all components. Substructure generated by hyperfine splitting accounted for some features recorded in the individual spectral scans. These results were not analyzed.

Both scalar,  $\alpha_0$ , and vector  $\alpha_2$ , polarizability terms were calculated from tuning curves such as those shown in Figs. 4 and 5. The experimental data were fit by least squares to the standard expression for the quadratic Stark effect,<sup>17</sup>

$$E = -\{\alpha_0 + \alpha_2[3J_z^2 - J(J+1)]/[J(2J-1)]\}V_s^2/2,$$

where  $V_s$  is the electric field strength.

Polarizabilities are tabulated in Table I. Drift of laser reference frequency during measurements provided the major contribution to the maximum error estimates listed in Table I. Data sets used to construct tuning curves were selected for optimum laser-frequency stability, judged on the basis of the positions recorded for the  $7d_{3/2}, J_z = \frac{3}{2}$  and  $7d_{5/2}, J_z = \frac{5}{2}$  components (which are nearly independent of field) in each scan of the  $\omega_2$  laser.

#### 5f spectroscopy

The  $5f$  resonances were also recorded in scans of the  $\omega_2$  laser, as shown in Fig. 3. For these spectra, the  $\text{CO}_2$  laser

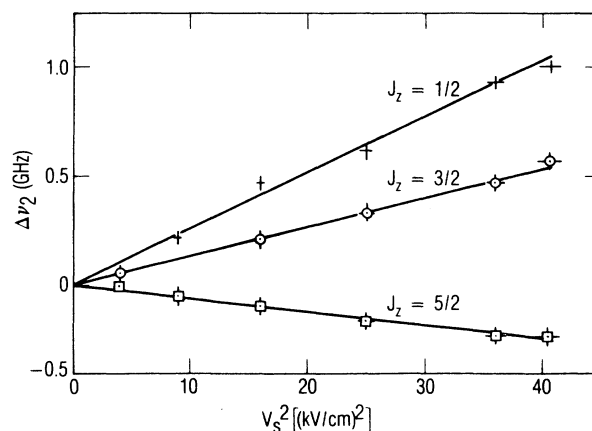


FIG. 4. Stark-tuning curve for  $7d_{5/2}$ . The solid straight lines are drawn for reference. Abscissa values should be multiplied by a correction factor of 1.029.

frequency was held constant, while the  $\omega_2$  dye-laser frequency was scanned. The electric field was incremented between successive  $\omega_2$  scans. The three-photon transition to the more polarizable  $5f$  state, induced by the  $\text{CO}_2$  laser, appears in the right-hand components. This transition split into the expected  $J_z$  manifolds when the electric field was applied. The tuning data are plotted as a function of  $V_s^2$  for  $5f_{7/2}$  in Fig. 5. The polarizabilities in Table I are corrected for the slight shift of the  $7d$  levels.

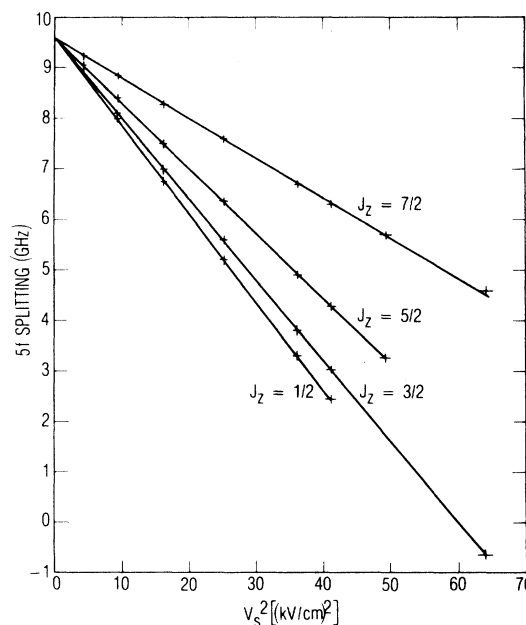


FIG. 5. Stark-tuning curve for  $5f_{7/2}$ . The solid straight lines are drawn for reference. Abscissa values should be multiplied by a correction factor of 1.029. The ordinate is the frequency splitting between the  $5d_{5/2} J_z = \frac{5}{2}$  component, which is nearly stationary, and the  $5f$  component indicated on the figure.

TABLE I. Polarizabilities for two states of cesium in units of  $a_0^3$ .

Cesium $7d$				
	$J = \frac{3}{2}$		$J = \frac{5}{2}$	
	$\alpha_0$	$\alpha_2$	$\alpha_0$	$\alpha_2$
Measured	$-6.0(8) \times 10^4$	$6.6(3) \times 10^4$	$-7.6(8) \times 10^4$	$1.29(4) \times 10^5$
Calculated	$-6.64 \times 10^4$	$-1.45 \times 10^4$	$-6.64 \times 10^4$	$1.23 \times 10^5$
Cesium $5f$				
	$J = \frac{5}{2}$		$J = \frac{7}{2}$	
	$\alpha_0$	$\alpha_2$	$\alpha_0$	$\alpha_2$
Measured	$1.08(2) \times 10^6$	$-3.9(1) \times 10^5$	$1.12(2) \times 10^6$	$-4.3(1) \times 10^5$
Calculated	$1.11 \times 10^6$	$-3.94 \times 10^5$	$1.11 \times 10^6$	$-3.70 \times 10^5$

## Autler-Townes splitting

As the electric field is increased,  $J_z$  components of the  $5f$  terms approach the  $7d$  resonance, as shown in Fig. 6. Both  $5f$  and  $7d$  components intensify near resonance, as shown in Fig. 3 (compare the spectrum recorded at 6 kV at gain  $\frac{1}{3}$  with the spectrum at 5 kV/cm recorded with unit gain). Spectra observed in interaction regions are shown in greater detail in Fig. 7. Both components share equal intensity near the point of avoided crossing. The minimum separation, observed at the crossing point, is indicative of the Autler-Townes interaction. As discussed above, these results are readily understood in terms of the model for Autler-Townes (AT) interaction, whereby the  $7d$  state, dressed by the  $\text{CO}_2$  laser photon, interacts with the  $5f$  state. The minimum splitting between AT components should be proportional to the Rabi frequency,  $\mu \cdot \epsilon / \hbar$ , where  $\mu$  is the transition dipole matrix element and  $\epsilon$  is the optical-field strength. Therefore the Rabi frequency, and the minimum AT splitting, are proportional to the square root of  $\text{CO}_2$  laser intensity, provided the simple two-level AT model is applicable to the four-level

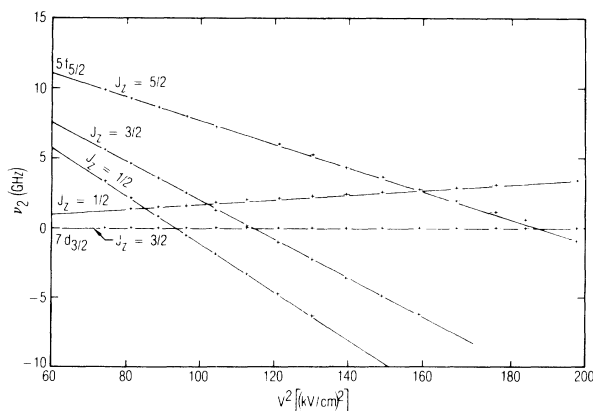


FIG. 6. Stark-tuning curves for  $5f_{5/2}$  in the region of  $7d_{3/2}$  resonance. The solid straight lines are drawn for reference. Abscissa values should be multiplied by a correction factor of 1.029.

system. In Fig. 8, the observed values for various minimum AT splittings, corresponding to different  $J_z$  components, are plotted as a function of the Clebsch-Gordan (CG) coefficients that connect the  $7d$  and  $5f$  components,

$$\begin{pmatrix} J & 1 & J' \\ -J_z & -\Delta J_z & J'_z \end{pmatrix}.$$

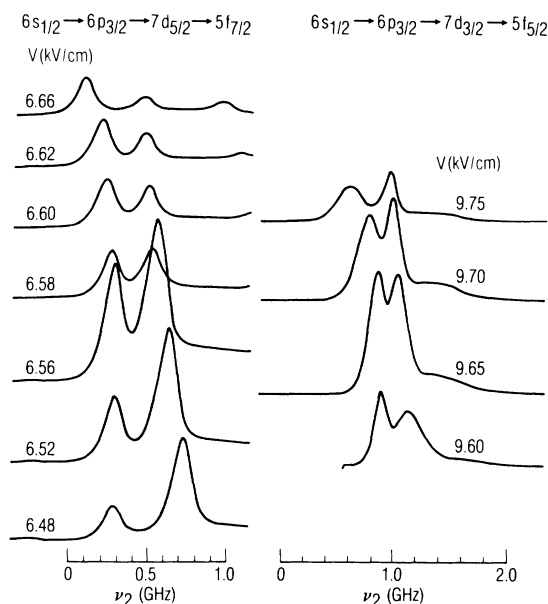


FIG. 7. Spectral scans recorded as a function of  $\nu_2$  for  $6s_{1/2}-6p_{3/2}-7d_{5/2}-5f_{7/2}$  in the region of  $7d_{5/2}$  resonance and of  $\nu_2$  for  $6s_{1/2}-6p_{3/2}-7d_{3/2}-5f_{5/2}$  in the region of  $7d_{3/2}$  resonance. In both sets of spectra the  $7d$  component appears on the left at low field and shifts slightly to higher frequency at high fields. The  $5f$  component appears on the right at low fields and shifts rapidly to lower energy for high fields. Thus, the left component at the highest field is principally  $5f$ . Gain was reduced by a factor of 3 for  $7d_{5/2}-5f_{7/2}$  scans at 6.58–6.66 kV/cm.

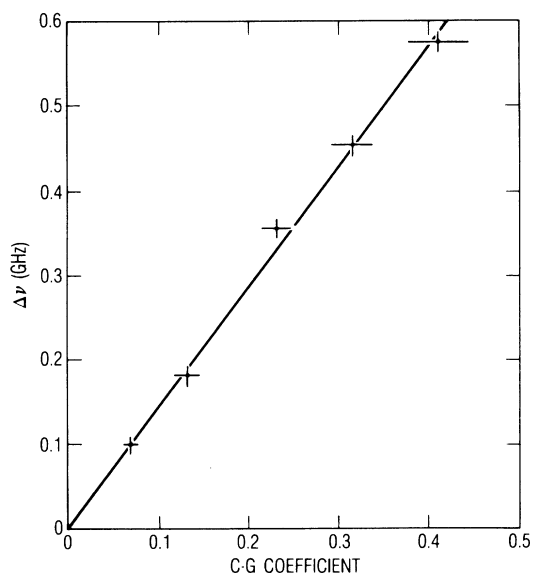


FIG. 8. Minimum Autler-Townes splitting for  $7d$ - $5f$  transitions vs the Clebsch-Gordan coefficient.

The laser intensities were maintained constant for these measurements, so that the Rabi frequency should be directly proportional to the CG coefficient. This was observed, as shown in Fig. 8. (It was not readily feasible to vary the  $\text{CO}_2$  laser beam intensity without changing other beam parameters.) Additional measurements demonstrated that the splitting pattern and tuning curves were independent of dye-laser intensities. Some tuning curves for interaction regions, such as that shown in Fig. 6 for  $6s_{1/2}$ - $6p_{3/2}$ - $7d_{3/2}$ - $5f_{5/2}$ , displayed substantially larger linewidths for the  $5f$  component than for the  $7d$  component. We observed similar linewidths in  $J_z = \frac{1}{2}$ - $\frac{3}{2}$  and  $J_z = \frac{3}{2}$ - $\frac{1}{2}$  transitions. The respective CG coefficients are 0.316 and 0.129. This rules out explanations of linewidths based on radiative interaction strength. The difference can be attributed to the larger polarizability for  $5f$ , which results in larger field inhomogeneity broadening. At the avoided crossing point, both components have comparable Stark-tuning slopes, thus explaining the observed equal linewidths at the crossing voltage.

#### Forbidden transition

In Fig. 9, tuning curves are presented for the transition  $7d_{3/2}$ ,  $J_z = \frac{1}{2}$ - $5f_{5/2}$ ,  $J_z = \frac{5}{2}$ . Distinct intensification of the  $5f_{5/2}$ ,  $J_z = \frac{5}{2}$  component is observed in the region of  $7d_{3/2}$ ,  $J_z = \frac{1}{2}$ . There is no indication of an avoided crossing. The fluorescence signals were linearly dependent on  $\text{CO}_2$  laser intensity and dye laser intensity.

#### DISCUSSION

The measured  $7d$  polarizabilities can be compared to values calculated from oscillator strengths estimated by

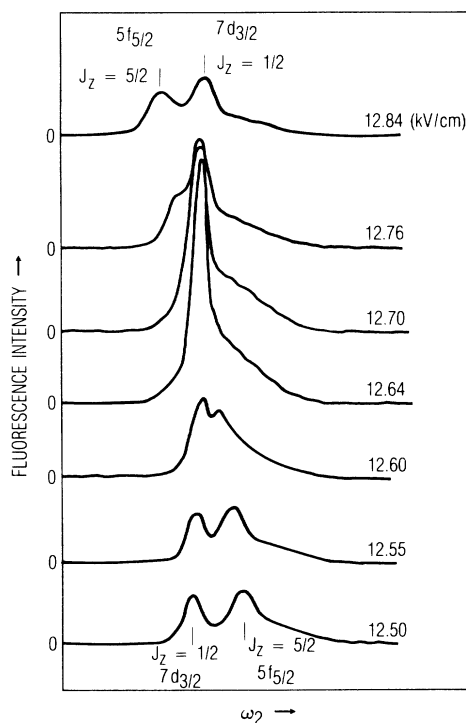


FIG. 9. Intensification and crossing of  $5f_{5/2}$ ,  $J_z = \frac{5}{2}$  and  $7d_{3/2}$ ,  $J_z = \frac{1}{2}$  components.

Anderson and Zilitis<sup>18</sup> using the Bates-Daamgard approximation (Table I). Corresponding values agree, nearly within experimental error, for the  $7d_{5/2}$  levels, but the  $7d_{3/2}$  value for  $\alpha_2$  differs by many times the experimental error. The calculated values are based on  $LS$ -coupling schemes. Therefore they are particularly inaccurate for cesium, which has appreciable spin-orbit coupling. The experimental values are expected to be more reliable.

Level energies measured for  $7d$  agree, within experimental error, with those reported by O'Sullivan and Stoicheff<sup>19</sup> and those extrapolated to zero field for the  $5f$  are within experimental error of those reported by Erickson and Wenaker.<sup>20</sup>

The  $5f$  polarizability derives primarily from interaction with the  $5g$  state. This permits accurate estimation of the oscillator strength connecting  $5f$  and  $5g$  states. The average measured value is  $f = 0.0336 \pm 0.0003$ , in close agreement with the value of 0.0344, estimated by Anderson and Zilitis.<sup>20</sup> ( $f$  was calculated from  $f = 4\pi\alpha/r_0\lambda^2$ , where  $\alpha$  is the polarizability for  $5f_{5/2}$ ,  $r_0$  is the classical electron radius,  $\lambda$  is the wavelength of the  $5f$ - $5g$  transition, and all quantities are converted to consistent units.) This is a case where the Stark effect provides both superior accuracy and ease of measurement compared to direct optical methods. (To the best of our knowledge there are no direct optical measurements of  $f$  for Cs  $5f$ - $5g$ .)

The appearance of the  $7d$  resonance in all spectral scans, including those recorded at voltages far from  $5f$  resonance conditions, is due to a blackbody excitation process. The  $7d$  resonance is observed, even in the absence of  $\text{CO}_2$  laser excitation, although the monitored fluorescence originates from a state at higher energy than  $7d$  (either  $5f$

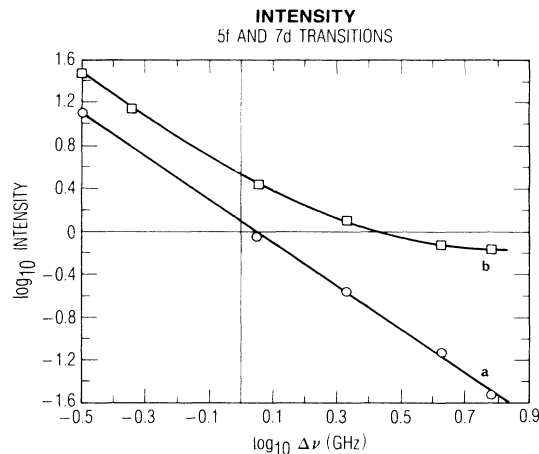


FIG. 10.  $\log_{10}$  of intensity for curve *a*,  $5f_{7/2}$ ,  $J_z = \frac{1}{2}$  and for curve *b*,  $7d_{5/2}$ ,  $J_z = \frac{1}{2}$  components vs  $\log_{10}$  of their frequency separation from the nominal crossing frequency.

or  $8p$ , depending on the experiment). Based on the large oscillator strength of the  $7d$ - $5f$  transition, we estimate a substantial blackbody excitation rate from  $7d$  to  $5f$ , in agreement with the observed  $5d$  signal. We can separate contributions to the signals from laser and blackbody sources by examining the intensity of the  $7d$  and  $5f$  components as a function of their separation (denoted  $\Delta\nu$ ) from the (avoided) crossing point frequency. When  $\Delta\nu=0$ , the laser source is in resonance with the unperturbed  $7d$  and  $5f$  states, therefore there should be maximum interaction and intensification. The data are displayed on a log-log plot in Fig. 10. The  $5f$  component (curve *a*) is described by a straight line with slope  $-2.0$  in the figure. This is consistent with a Lorentzian, power-broadened line shape for laser-induced transition to the final  $5f$  state. Curve *b* of Fig. 10, representing intensity of the  $7d$  component, is well described by the sum of a Lorentzian and a frequency-independent blackbody contribution, as shown by the calculated solid curve, labeled *b* in Fig. 10.

The blackbody-induced signal is overwhelmed when the  $7d$ - $5f$  resonance condition is satisfied. The strong optical interaction for this transition is manifested in both the in-

tensification, and in the magnitude of the avoided crossing, displayed in Fig. 7. The linear dependence of splitting on the Rabi frequency for the  $\omega_3$  transition suggests that the four-level Autler-Townes split system behaves similar to a simple two-level system. The additional complications associated with four-level interactions are not evident, even when the  $\omega_1$  and  $\omega_2$  Rabi frequencies are on the order of two-tenths those for  $\omega_3$ .

The presence of the angular momentum forbidden  $7d_{3/2}$ ,  $J_z = \frac{1}{2}$ - $5f_{5/2}$ ,  $J_z = \frac{5}{2}$  transition can be explained on the basis of higher-order dc Stark terms that mix  $5f_{5/2}$ ,  $J_z = \frac{5}{2}$  with  $5f_{5/2}$ ,  $J_z = \frac{3}{2}$  and  $J_z = \frac{1}{2}$ . These terms are quadratic in the applied electric field and are significant due to proximity of  $5g$ . Although the  $7d_{3/2}$ ,  $J_z = \frac{1}{2}$ - $5f_{7/2}$ ,  $J_z = \frac{5}{2}$  transition appears to be intense, when its intensity is properly normalized to the allowed transitions, such as  $J_z = \frac{1}{2}$ - $J_z = \frac{3}{2}$ , the forbidden transition is found to be weaker by a factor of about  $1 \times 10^{-5}$ . The apparent strength arises from the fact that the allowed transitions are strongly saturated under experimental conditions. Based on the  $38 \text{ cm}^{-1}$  separation of the  $5f$  and  $5g$  levels and on an oscillator strength of 0.034, we estimate an angular momentum mixing coefficient of  $6 \times 10^{-6}$  for the  $5f_{7/2}$  and  $5f_{5/2}$  states at a field of 12.5 kV/cm, in agreement with the observed intensity.

In conclusion, three-photon resonant spectroscopy of cesium  $5f$  states reveals Autler-Townes interactions and Stark-tuning behavior consistent with results previously observed for lower-energy states by one-photon and two-photon techniques. The three-photon technique facilitates high-resolution studies in a thermal cell. The resultant cesium Stark spectroscopy is generally typical of a light one-electron atom, with the exception that the polarizabilities show some deviations from  $LS$  coupling. In the  $5f$  state Stark interactions are clearly dominated by near-degenerate interaction with the  $5g$  manifold.

#### ACKNOWLEDGMENT

We wish to acknowledge the excellent technical support provided by Kevin Kell and valuable discussions concerning interpretation of results with Dr. James Camparo. This work was supported by the Aerospace Sponsored Research program through the Aerospace Corporation.

\*Send correspondence to this author.

†Present address: Rockwell Science Center, Thousand Oaks, California.

<sup>1</sup>N. Lu, P. R. Berman, A. G. Yodh, Y. S. Bai, and T. W. Mossberg, *Phys. Rev. A* **33**, 395 (1986).

<sup>2</sup>C. Y. Tai, C. C. Kim, R. T. Deck, and Y. T. Wu, *Phys. Rev. A* **33**, 3970 (1986).

<sup>3</sup>A. I. Burshtein, *Zh. Eksp. Teor. Fiz.* **48**, 850 (1965) [*Sov. Phys.—JETP* **21**, 567 (1965)].

<sup>4</sup>A. I. Burshtein, *Zh. Eksp. Teor. Fiz.* **49**, 1362 (1965) [*Sov. Phys.—JETP* **22**, 939 (1966)].

<sup>5</sup>M. Newstein, *Phys. Rev.* **167**, 89 (1968).

<sup>6</sup>B. R. Mollow, *Phys. Rev.* **188**, 1969 (1969).

<sup>7</sup>F. Schuda, C. R. Stroud, Jr., and M. Hercher, *J. Phys. B* **7**, L198 (1974).

<sup>8</sup>H. Walther, *Bull. Am. Phys. Soc. II* **20**, 1467 (1975).

<sup>9</sup>H. Walther, *Laser Spectroscopy*, edited by S. Haroche, J. C. Pebay-Peyroula, T. W. Hansch, and S. E. Harris (Springer Verlag, Berlin, 1975).

<sup>10</sup>F. Y. Wu, R. E. Grove, and S. Ezekiel, *Phys. Rev. Lett.* **35**, 1426 (1975).

<sup>11</sup>R. E. Grove, E. Y. Grove, F. Y. Wu, and S. Ezekiel, *Phys. Rev. A* **15**, 227 (1977).

<sup>12</sup>J. L. Picque and J. Pinard, *J. Phys. B* **9**, L77 (1976).

- <sup>13</sup>C. Delsart and J. C. Keller, *J. Phys. B* **9**, 2769 (1976).
- <sup>14</sup>H. R. Gray and C. R. Stroud, Jr., *Opt. Commun.* **25**, 259 (1978).
- <sup>15</sup>K. Fredriksson, H. Lundberg, and S. Svanberg, *Phys. Rev. A* **21**, 241 (1980).
- <sup>16</sup>T. F. Gallagher and W. E. Cooke, *Phys. Rev. A* **18**, 2510 (1978).
- <sup>17</sup>A. Khadjavi, A. Lurio, and W. Happer, *Phys. Rev.* **167**, 128 (1968).
- <sup>18</sup>E. M. Anderson and V. A. Zilitis, *Opt. Spektrosk.* **16**, 382 (1964) [*Opt. Spectrosc. (USSR)* **16**, 211 (1964)].
- <sup>19</sup>M. S. O'Sullivan and B. P. Stoicheff, *Can. J. Phys.* **61**, 940 (1983).
- <sup>20</sup>K. B. S. Ericksson and I. Wenaker, *Phys. Scr.* **1**, 21 (1970).